

Estimate of $\mathcal{B}(\bar{B} \rightarrow X_s \gamma)$ at $\mathcal{O}(\alpha_s^2)$

M. Misiak,^{1,2} H. M. Asatrian,³ K. Bieri,⁴ M. Czakon,⁵ A. Czarnecki,⁶ T. Ewerth,⁴
 A. Ferroglia,⁷ P. Gambino,⁸ M. Gorbahn,⁹ C. Greub,⁴ U. Haisch,¹⁰ A. Hovhannisyanyan,³
 T. Hurth,^{2,11} A. Mitov,¹² V. Poghosyan,³ M. Ślusarczyk,⁶ and M. Steinhauser⁹

¹*Institute of Theoretical Physics, Warsaw University, PL-00-681 Warsaw, Poland*

²*Theoretical Physics Division, CERN, CH-1211 Geneva 23, Switzerland*

³*Yerevan Physics Institute, 375036 Yerevan, Armenia*

⁴*Institut für Theoretische Physik, Universität Bern, CH-3012 Bern, Switzerland*

⁵*Institut für Theoretische Physik und Astrophysik,
 Universität Würzburg, D-97074 Würzburg, Germany*

⁶*Department of Physics, University of Alberta, AB T6G 2J1 Edmonton, Canada*

⁷*Physikalisches Institut, Albert-Ludwigs-Universität, D-79104 Freiburg, Germany*

⁸*INFN, Torino & Dipartimento di Fisica Teorica, Università di Torino, I-10125 Torino, Italy*

⁹*Institut für Theoretische Teilchenphysik, Universität Karlsruhe (TH), D-76128 Karlsruhe, Germany*

¹⁰*Institut für Theoretische Physik, Universität Zürich, CH-8057 Zürich, Switzerland*

¹¹*SLAC, Stanford University, Stanford, CA 94309, USA*

¹²*Deutsches Elektronen-Synchrotron DESY, D-15738 Zeuthen, Germany*

(Dated: September 18, 2006)

Combining our results for various $\mathcal{O}(\alpha_s^2)$ corrections to the weak radiative B -meson decay, we are able to present the first estimate of the branching ratio at the next-to-next-to-leading order in QCD. We find $\mathcal{B}(\bar{B} \rightarrow X_s \gamma) = (3.15 \pm 0.23) \times 10^{-4}$ for $E_\gamma > 1.6$ GeV in the \bar{B} -meson rest frame. The four types of uncertainties: nonperturbative (5%), parametric (3%), higher-order (3%) and m_c -interpolation ambiguity (3%) have been added in quadrature to obtain the total error.

PACS numbers: 12.38.Bx, 13.20.He

The inclusive radiative B -meson decay provides important constraints on the minimal supersymmetric standard model and many other theories of new physics at the electroweak scale. The power of such constraints depends on the accuracy of both the experiments and the standard model (SM) calculations. The latest measurements by Belle and BABAR are reported in Refs. [1, 2]. The world average performed by the Heavy Flavor Averaging Group [3] for $E_\gamma > 1.6$ GeV reads

$$\mathcal{B}(\bar{B} \rightarrow X_s \gamma) = (3.55 \pm 0.24^{+0.09}_{-0.10} \pm 0.03) \times 10^{-4}. \quad (1)$$

The combined error in the above result is of the same size as the expected $\mathcal{O}(\alpha_s^2)$ next-to-next-to-leading order (NNLO) QCD corrections to the perturbative decay width $\Gamma(b \rightarrow X_s^{\text{parton}} \gamma)$, and larger than the known nonperturbative corrections to the relation $\Gamma(\bar{B} \rightarrow X_s \gamma) \simeq \Gamma(b \rightarrow X_s^{\text{parton}} \gamma)$ [4]–[6]. Thus, calculating the SM prediction for the b -quark decay rate at the NNLO is necessary for taking full advantage of the measurements.

Evaluating the $\mathcal{O}(\alpha_s^2)$ corrections to $\mathcal{B}(b \rightarrow X_s^{\text{parton}} \gamma)$ is a very involved task because hundreds of three-loop on-shell and thousands of four-loop tadpole Feynman diagrams need to be computed. In a series of papers [7]–[14], we have presented partial contributions to this enterprise. The purpose of the present Letter is to combine all the existing results and obtain the first estimate of the branching ratio at the NNLO. We call it an estimate rather than a prediction because some of the numerically important contributions have been found using an interpolation in the charm quark mass, which introduces uncertainties that are difficult to quantify.

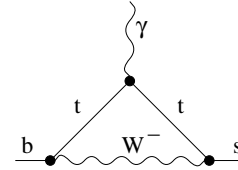


FIG. 1: Sample LO diagram for the $b \rightarrow s \gamma$ transition.

Let us begin with recalling that the leading-order (LO) contribution to the considered decay originates from one-loop diagrams in the SM. An example of such a diagram is shown in Fig. 1. Dressing this diagram with one or two virtual gluons gives examples of diagrams that one encounters at the next-to-leading order (NLO) and the NNLO. In addition, one should include diagrams describing the bremsstrahlung of gluons and light quarks.

An additional difficulty in the analysis of the considered decay is the presence of large logarithms $(\alpha_s \ln M_W^2/m_b^2)^n$ that should be resummed at each order of the perturbation series in α_s . To do so, one employs a low-energy effective theory that arises after decoupling the top quark and the heavy electroweak bosons. Weak interaction vertices (operators) in this theory are either of dipole type ($\bar{s} \sigma^{\mu\nu} b F_{\mu\nu}$, $\bar{s} \sigma^{\mu\nu} T^a b G_{\mu\nu}^a$) or contain four quarks ($[\bar{s} \Gamma b][\bar{q} \Gamma' q]$). Coupling constants at these vertices (Wilson coefficients) are first evaluated at the electroweak renormalization scale $\mu_0 \sim m_t, M_W$ by solving the so-called *matching* conditions. Next, they are evolved down to the low-energy scale $\mu_b \sim m_b$

according to the effective theory renormalization group equations (RGE). The RGE are governed by the operator *mixing* under renormalization. Finally, one computes the *matrix elements* of the operators, which in our case amounts to calculating on-shell diagrams with single insertions of the effective theory vertices.

A summary of the $\bar{B} \rightarrow X_s \gamma$ calculation status before the beginning of our project can be found, e.g., in Ref. [15]. At the NNLO level, the dipole and the four-quark operators need to be matched up to three and two loops, respectively. Renormalization constants up to four loops must be found for $b \rightarrow s\gamma$ and $b \rightarrow sg$ diagrams with four-quark operator insertions, while three-loop mixing is sufficient in the remaining cases. Two-loop matrix elements of the dipole operators and three-loop matrix elements of the four-quark operators must be evaluated in the last step.

Three-loop dipole operator matching was found in Ref. [8]. The necessary three-loop mixing was calculated in Ref. [9]. The four-loop mixing was evaluated in Ref. [13]. Two-loop matrix element of the photonic dipole operator together with the corresponding bremsstrahlung was found in Refs. [10, 11] and recently confirmed in Ref. [12]. Three-loop matrix elements of the four-quark operators were found in Ref. [7] within the so-called large- β_0 approximation. A calculation that goes beyond this approximation by employing an interpolation in the charm quark mass m_c has just been completed in Ref. [14].

With all these results at hand, we are ready to present the first estimate of the $\bar{B} \rightarrow X_s \gamma$ branching ratio at $\mathcal{O}(\alpha_s^2)$. It reads [23]

$$\mathcal{B}(\bar{B} \rightarrow X_s \gamma) = (3.15 \pm 0.23) \times 10^{-4}, \quad (2)$$

for $E_\gamma > 1.6$ GeV in the \bar{B} -meson rest frame. The four types of uncertainties: nonperturbative (5%), parametric (3%), higher-order (3%) and m_c -interpolation ambiguity (3%) have been added in quadrature in Eq. (2).

The central value in Eq. (2) was obtained for $\mu_0 = 160$ GeV, $\mu_b = 2.5$ GeV and $\mu_c = 1.5$ GeV. The latter quantity stands for the charm mass $\overline{\text{MS}}$ renormalization scale that is allowed to be different from μ_b . The branching ratio dependence on each of the three scales is shown in Fig. 2. Once one of them is varied, the remaining two are fixed at the values that have been mentioned above. The reduction of the renormalization scale dependence at the NNLO is clearly seen. The most pronounced effect occurs for μ_c that was the main source of uncertainty at the NLO. (The LO results are m_c - and thus μ_c -independent.) The current uncertainty of $\pm 3\%$ due to higher-order [$\mathcal{O}(\alpha_s^3)$] effects is estimated from the NNLO curves in Fig. 2.

The reference value of $\mu_b = 2.5$ GeV that we have chosen is roughly twice smaller than in the previous LO and NLO analyses. Given the stability of the NNLO result for large values of μ_b , we do not underestimate any uncertainty from that region. Furthermore, because the center-of-mass energy $m_B \simeq 5.3$ GeV gets

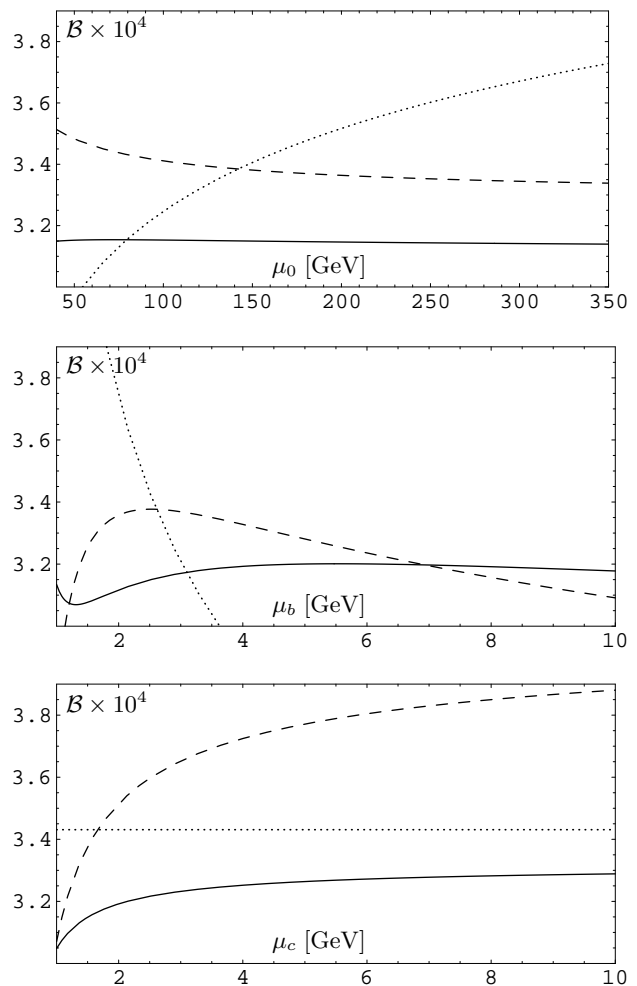


FIG. 2: Renormalization scale dependence of $\mathcal{B}(\bar{B} \rightarrow X_s \gamma)$ in units 10^{-4} at the LO (dotted lines), NLO (dashed lines) and NNLO (solid lines). The plots describe subsequently the dependence on the matching scale μ_0 , the low-energy scale μ_b , and the charm mass renormalization scale μ_c .

distributed among various partons, the reference value of $\mu_b = 2.5$ GeV seems reasonable. Lower values of μ_b have an advantage of making μ_c -stabilization more efficient because the NNLO logarithm that compensates μ_c -dependence of the NLO amplitude comes multiplied by $\alpha_s(\mu_b)$.

The $\pm 3\%$ uncertainty that is assigned to the m_c -interpolation ambiguity has been estimated studying by how much the NNLO branching ratio depends on various interpolation assumptions. More details on this point and other elements of the phenomenological analysis (including the input parameters) can be found in Ref. [14].

As far as the parametric uncertainties are concerned, the dominant ones come from $\alpha_s(M_Z)$ ($\pm 2.0\%$) and the measured semileptonic branching ratio $\mathcal{B}(\bar{B} \rightarrow X_c e \bar{\nu})$ ($\pm 1.6\%$) to which we normalize. The third-to-largest uncertainty ($\pm 1.1\%$) is due to the correlated errors in

$m_c(m_c)$ and the semileptonic phase-space factor

$$C = \left| \frac{V_{ub}}{V_{cb}} \right|^2 \frac{\Gamma[\bar{B} \rightarrow X_c e \bar{\nu}]}{\Gamma[\bar{B} \rightarrow X_u e \bar{\nu}]} \quad (3)$$

The factor C has been determined in Ref. [16] together with $m_c(m_c)$ from a global fit to the semileptonic data. If the normalization to $\mathcal{B}(\bar{B} \rightarrow X_c e \bar{\nu})$ was not applied in the $\bar{B} \rightarrow X_s \gamma$ calculation, the error due to $m_c(m_c)$ would amount to $\pm 2.8\%$. At the same time, one would need to take into account uncertainties in m_b^5 and the Cabibbo-Kobayashi-Maskawa factor $|V_{ts}^* V_{tb}|^2$, each of which exceeds $\pm 3\%$.

The nonperturbative uncertainty in Eq. (2) is due to matrix elements of the four-quark operators in the presence of one gluon that is not soft ($Q^2 \sim m_b^2, m_b \Lambda$, where $\Lambda \sim \Lambda_{\text{QCD}}$). Unknown nonperturbative corrections to them scale like $\alpha_s \Lambda / m_b$ in the limit $m_c \ll m_b/2$ and like $\alpha_s \Lambda^2 / m_c^2$ in the limit $m_c \gg m_b/2$. Because $m_c < m_b/2$ in reality, $\alpha_s \Lambda / m_b$ should be considered as the quantity that sets the size of such effects. Consequently, a $\pm 5\%$ nonperturbative uncertainty has been assigned to the result in Eq. (2). This is the dominant uncertainty at present. Thus, a detailed analysis of such effects would be more than welcome. So far, no published results on this issue exist. Even lacking a trustworthy method for calculating such effects, it might be possible to put rough upper bounds on them that could supersede the current guess-estimate of $\pm 5\%$. Nonperturbative corrections to inclusive $\bar{B} \rightarrow X_{d,s} \gamma$ decays that scale like Λ / m_b may arise when the b -quark annihilation vertex does not coincide with the hard photon emission vertex; see, e.g., Ref. [6] or comments on $\bar{B} \rightarrow X_d \gamma$ in Sec. 2 of Ref. [5].

The NNLO central value in Eq. (2) differs from some of the previous NLO predictions by between 1 and 2 error bars of the NLO results. Because those error bars were obtained by adding various theoretical uncertainties in quadrature, such a shift is not improbable, similarly to shifts by less than 2σ in experimental results. The shift from the NLO to the NNLO level diminishes with lowering the value of μ_c , which has motivated us to use the relatively low $\mu_c = 1.5$ GeV as a reference value here.

The NNLO results turn out to be only marginally dependent on whether one follows (or not) the approach of Ref. [17] where the top-quark contribution to the decay amplitude was calculated separately and rescaled by quark mass ratios to improve convergence of the perturbation series. Although the top contribution alone indeed behaves better also at the NNLO level when such an approach is used, the charm quark contribution (to which no rescaling has been applied in Ref. [17]) does not turn out to be particularly stable beyond the NLO. Consequently, in the derivation of Eq. (2) and Fig. 2, we have used the simpler method of treating charm and top sectors together.

Our result in Eq. (2) has been obtained under the assumption that the photonic dipole operator contribution to the integrated E_γ spectrum below 1.6 GeV is well approximated by a fixed-order perturbative calculation (see

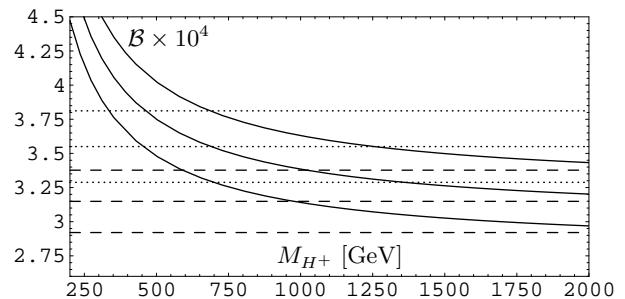


FIG. 3: $\mathcal{B}(\bar{B} \rightarrow X_s \gamma)$ as a function of the charged Higgs boson mass in the THDM II for $\tan \beta = 2$ (solid lines). The dashed and dotted lines show the SM and experimental results, respectively (see the text).

Note added). For lower values of the photon energy cut, the following numerical fit can be used:

$$\left(\frac{\mathcal{B}(E_\gamma > E_0)}{\mathcal{B}(E_\gamma > 1.6 \text{ GeV})} \right)_{\text{fixed order}} \simeq 1 + 0.15x - 0.14x^2, \quad (4)$$

where $x = 1 - E_0 / (1.6 \text{ GeV})$. This formula coincides with our NNLO results up to $\pm 0.1\%$ for $E_0 \in [1.0, 1.6]$ GeV. The error is practically E_0 -independent in this range.

In the remainder of this Letter, we shall update the $\bar{B} \rightarrow X_s \gamma$ constraints on the charged Higgs boson mass in the two-Higgs-doublet-model II (THDM II) [18]. The solid lines in Fig. 3 show the dependence of $\mathcal{B}(\bar{B} \rightarrow X_s \gamma)$ on this mass when the ratio of the two vacuum expectation values, $\tan \beta$, is equal to 2. The dashed and dotted lines show the SM (NNLO) and the experimental results, respectively. In each case, the middle line is the central value, while the other two lines indicate uncertainties that one obtains by adding all the errors in quadrature.

In our THDM calculation, matching of the Wilson coefficients at the electroweak scale is complete up to the NLO [19], but the NNLO terms contain only the SM contributions (the THDM ones remain unknown). In consequence, the higher-order uncertainty becomes somewhat larger. This effect is estimated by varying the matching scale μ_0 from half to twice its central value. It does not exceed $\pm 1\%$ for the M_{H+} range in Fig. 3.

Even though the experimental result is above the SM one, the lower bound on M_{H+} for a generic value of $\tan \beta$ remains stronger than what one can derive from any other currently available measurement. If all the uncertainties are treated as Gaussian and combined in quadrature, the 95% (99%) CL bound amounts to around 295 (230) GeV. It is found for $\tan \beta \rightarrow \infty$ but stays practically constant down to $\tan \beta \simeq 2$. For smaller $\tan \beta$, the branching ratio and the bound on M_{H+} increase.

The contour plot in Fig. 4 shows the dependence of the M_{H+} bound on the experimental central value and error. The current experimental result (1) is indicated by the black square. Consequences of the future upgrades in the measurements will easily be read out from the plot, so long as no progress on the theoretical side is made. Of

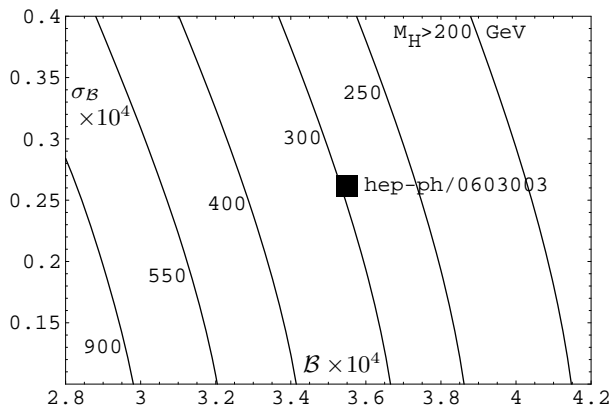


FIG. 4: The 95% CL lower bound on M_{H^+} as a function of the experimental central value (horizontal axis) and error (vertical axis). The experimental result from Eq. (1) is indicated by the black square. The contour lines represent values that lead to the same bound.

course, the derived bounds should be considered illustrative only because they depend very much on the theory uncertainties that have no statistical interpretation.

To conclude, we have provided the first estimate of $\mathcal{B}(\bar{B} \rightarrow X_s \gamma)$ at $\mathcal{O}(\alpha_s^2)$. The inclusion of the NNLO QCD corrections leads to a significant suppression of the branching ratio renormalization scale dependence that has been the main source of uncertainty at the NLO.

The central value is shifted downward with respect to all the previously published NLO results. It is now about 1σ lower than the experimental average (1). The dominant theoretical uncertainty is currently due to the unknown $\mathcal{O}(\alpha_s \Lambda/m_b)$ nonperturbative effects. In the two-Higgs-doublet model II, the experimental results favor a charged Higgs boson mass of around 650 GeV. The 95% C.L. bound for this mass amounts to around 295 GeV if all the uncertainties are treated as Gaussian.

We acknowledge support from the DFG through SFB/TR 9 and a Heisenberg contract, MIUR under Contract No. 2004021808-009, the Swiss National Foundation and RTN, BBW-Contract No. 01.0357, EU-Contracts No. HPRN-CT-2002-00311 and No. MTRN-CT-2006-035482, Polish KBN grant No. 2 P03B 078 26, the ANSEF N 05-PS-hepht-0825-338 program, Science and Engineering Research Canada, as well as a research fellowship and the Sofja Kovalevskaja Award of the Alexander von Humboldt Foundation.

Note added— Recently, our results from Eqs. (2) and (4) were combined in Ref. [20] with perturbative cutoff-related corrections that go beyond a fixed-order calculation [20, 21]. Because these corrections for $E_0 \leq 1.6$ GeV do not exceed our higher-order uncertainty of $\pm 3\%$, we postpone their consideration to a future upgrade of the phenomenological analysis, where other contributions of potentially the same size are going to be included, too (see Sec. 1 of Ref. [22]).

-
- [1] P. Koppenburg *et al.* (Belle Collaboration), Phys. Rev. Lett. **93**, 061803, (2004).
- [2] B. Aubert *et al.* (BABAR Collaboration), Phys. Rev. D **72**, 052004 (2005); B. Aubert *et al.* (BABAR Collaboration), Phys. Rev. Lett. **97**, 171803 (2006).
- [3] E. Barberio *et al.* (HFAG), hep-ex/0603003.
- [4] A.F. Falk, M.E. Luke and M.J. Savage, Phys. Rev. D **49**, 3367 (1994); I.I. Bigi *et al.*, hep-ph/9212227; M.B. Voloshin, Phys. Lett. B **397**, 275 (1997); A. Khodjamirian *et al.*, Phys. Lett. B **402**, 167 (1997); Z. Ligeti, L. Randall and M.B. Wise, Phys. Lett. B **402**, 178, (1997); A.K. Grant, A.G. Morgan, S. Nussinov and R.D. Peccei, Phys. Rev. D **56** 3151, (1997).
- [5] G. Buchalla, G. Isidori and S. J. Rey, Nucl. Phys. B **511**, 594 (1998).
- [6] S. J. Lee, M. Neubert and G. Paz, hep-ph/0609224.
- [7] K. Bieri, C. Greub and M. Steinhauser, Phys. Rev. D **67**, 114019 (2003).
- [8] M. Misiak and M. Steinhauser, Nucl. Phys. B **683**, 277 (2004).
- [9] M. Gorbahn and U. Haisch, Nucl. Phys. B **713**, 291 (2005); M. Gorbahn, U. Haisch and M. Misiak, Phys. Rev. Lett. **95**, 102004 (2005).
- [10] K. Melnikov and A. Mitov, Phys. Lett. B **620**, 69 (2005).
- [11] I. Blokland, A. Czarnecki, M. Misiak, M. Ślusarczyk and F. Tkachov, Phys. Rev. D **72**, 033014 (2005).
- [12] H. M. Asatrian, A. Hovhannisyanyan, V. Poghosyan, T. Ewerth, C. Greub and T. Hurth, Nucl. Phys. B **749**, 325 (2006); H. M. Asatrian, T. Ewerth, A. Ferroglia, P. Gambino and C. Greub, Nucl. Phys. B **762**, 212 (2007).
- [13] M. Czakon, U. Haisch and M. Misiak, hep-ph/0612329.
- [14] M. Misiak and M. Steinhauser, hep-ph/0609241 [Nucl. Phys. B (to be published)].
- [15] T. Hurth, Rev. Mod. Phys. **75**, 1159 (2003); A. J. Buras and M. Misiak, Acta Phys. Polon. B **33**, 2597 (2002).
- [16] C. W. Bauer, Z. Ligeti, M. Luke, A. V. Manohar and M. Trott, Phys. Rev. D **70**, 094017 (2004); A. H. Hoang and A. V. Manohar, Phys. Lett. B **633**, 526 (2006).
- [17] P. Gambino and M. Misiak, Nucl. Phys. B **611**, 338 (2001).
- [18] L. F. Abbott, P. Sikivie and M. B. Wise, Phys. Rev. D **21**, 1393 (1980).
- [19] M. Ciuchini, G. Degrossi, P. Gambino and G. F. Giudice, Nucl. Phys. B **527**, 21 (1998); F. M. Borzumati and C. Greub, Phys. Rev. D **58**, 074004 (1998).
- [20] T. Becher and M. Neubert, hep-ph/0610067.
- [21] T. Becher and M. Neubert, Phys. Lett. B **633**, 739 (2006); Phys. Lett. B **637**, 251 (2006).
- [22] H. M. Asatrian, T. Ewerth, H. Gabrielyan and C. Greub, hep-ph/0611123.
- [23] The small (-0.35%) correction from the four-loop $b \rightarrow sg$ mixing diagrams is not included in our numerical results.